Waiting Cost based Network Investment Decision-making under Uncertainty

Xiaohe Yan, *Student Member*, Chenghong Gu, *Member, IEEE,* Hongcai Zhang, *Member, IEEE,* Furong Li, *Senior Member, IEEE* and Yonghua Song, *Fellow, IEEE*

***Abstract*—Traditional system investment decision is costly and hard to reverse. This is aggravated by uncertainties from flexible load and renewables (FLR), which impact the accuracy of network investment decisions and could trigger a high asset risk. Thus, system operators have the incentive to postpone network reinforcement, and 'wait and see' whether the request of investment can be reduced or delayed with new information.**

This paper proposes a novel method to evaluate network investment horizon deferral based on the trade-off between waiting profit and waiting cost under FLR uncertainties. Although deferring investment leads to waiting cost, it is worthy to wait if the cost is smaller than the waiting profits. To capture the impact of FLR uncertainties on system investment, nodal uncertainties are converted into branch flow uncertainties based on a combined cumulant and Gram-Charlier expansion method. The waiting cost is quantified by the options' cost based on real options method and waiting profit is from asset present value reduction due to the deferral. Thus, by paying waiting cost, current investment cost can be reserved until uncertainties are reduced to an acceptable level. The waiting time is evaluated by Sharp ratio and expected return, determined by the waiting cost and uncertainty level. The results show that paying waiting cost is an economical way to reduce the impact of uncertainty and avoid hastily investment.

***Index Terms*—Network planning, Uncertainty, Real Options, Long-run Incremental Cost**

I. Introduction

Boosted by the ambition of decarbonisation, renewable is expected to increase by 43% in the next 5 years worldwide, although it brings high uncertainty to the system [1]. Additionally, energy storage is expected to increase 8 times to 1.6GW by 2020 in the UK [2] and electric vehicles also increase significantly to 17 million by 2040 [3]. However, currently, 90% of electric vehicles are uncontrollable [4], which means their operation also brings uncertainty to the system.

On the one hand, these uncertainties from flexible load and renewables (FLR) poses significant impacts on system power flow peaks, which severely challenges investment horizon evaluation. Thus, FLR uncertainties become a significant investment deterrent. On the other hand, the impact of these uncertainties might be reduced due to the development of Internet of Things and AI by providing more accurate prediction and better control strategy. As a result, the pressure on power transmission can be reduced and the load growth rate would decrease, even sometimes becoming negative. Thus, the time to reinforcement horizon (TRH) of networks should be dynamic to address the impact of FLR uncertainty.

Conventionally, there are two main investment theories. One is from the cost-of-capital view [5], which evaluates the investment capital based on the marginal product and user costs. The other is the 'q theory' [6], which focuses on the marginal unit of capital relative to its replacement cost. These theories are based on net present value, which means the network must be invested after a certain year. Net present value is used in the long-run incremental cost pricing method, which is widely applied in the UK [7].

However, these methods fail to reflect the impact of risk resulting from uncertainty on future network investment.[8] To capture the impact, two main investment decision methods are . One is the weighted average cost of capital [9], which proportionately weights the capital from different categories of the investment. But it is not fair and efficient for network users due to the assumption of constant risk level [10]. Thus, the risk is adjusted in the rate of return. The other is the Real Options method [11], which augments the cost of occurred uncertainty, as options cost, with net present value [12]. Network operators could defer the investment and receive more information to reduce the uncertainty by paying the cost of options. This decision-making tool addresses the issue of irreversible investments by introducing the possibility that the network operator could pay the cost of options [13-15]. Paper [16] assesses the value of demand response based on the real options method considering uncertainties both in operation and planning. It also can be used to devise the optimal risk-averse investment policy for renewable generations [17]. The impacts from uncertainty resulting from renewables and load are converted as options cost, which is added on the present value in investment cost evaluation [18].

Uncertainty means that it is impossible to exactly describe the future FLR status because of limited information. Thus, forecast error is increasing over time, which means the uncertainty level is higher for further future. [19][20][21]The impact of uncertainty on load is approximated by applying a bigger load growth rate [22], which is not accurate to capture the behaviour of network users. Papers [23, 24] use the triple exponential smoothing to qualify the forecast errors of photovoltaic and wind power, which smooths time series data by assigning exponentially decreasing weights over time.

Currently, reinforcement horizon is determined by assessing the unused capacity of branches [7], which cannot reflect the impact of uncertainty. To determine whether the investment decision-making should be postponed, waiting cost, waiting profit and uncertainty level of the future should be determined. The expected return is evaluated to reflect the cost and profit in [25]. Considering the risks from renewables and flexible load, the risk-adjusted return on capital based on the Sharpe ratio is introduced in network management [26]. Jensen's measure [27] and Treynor ratio [28] also are widely used to describe the relationship between risk and return. But, Jensen's measure highly depends on average market return and Treynor ratio is evaluated based on the excess return of the unit risk.

This paper designs a novel decision-making scheme for network owners to avoid irreversible investment resulting from FLR uncertainties. Firstly, the uncertainties from FLR are converted into branch power flow by using the combined cumulant and Gram-Charlier expansion method. It directly links nodal uncertainty with system investment decision-making based on network power flow peaks. Thereafter, the cost and profit from investment deferral are evaluated on the annual basis based on the asset cost and FLR uncertainty. Waiting cost is represented by the cost of the options, derived from the real options method, meaning the current present value will be held for a certain period by paying the cost of options. Waiting profit is calculated from asset present value reduction due to the investment deferral. The expected return after waiting is the difference between waiting cost and profit. The deferral horizon under uncertainties is determined by the Sharpe ratio, decided by the uncertainty level and the trade-off between waiting cost and waiting profits. The proposed method is demonstrated on a UK GSP network and sensitivity analysis shows the impact of uncertainty levels.

This paper has three innovations. It: 1) introduces waiting cost, evaluated by real options based on risk-neutral theory, bringing more flexibility to investment decision-making under severe uncertainties; 2) addresses system reinforcement by dynamising reinforcement horizon, thus optimising network investment by receiving more information to reduce the impact from uncertainties; 3) improves investment decision-making by combining real options and Sharpe ratio, efficiently capturing the impact from uncertainties on future investment;

The rest of the paper is organised as follows: Section II gives the structure of challenges and solutions. Section III dives the probabilistic power flow based on combined cumulant and Gram-Charlier expansion method. Section IV designs the network investment decision-making model. Sections V and VI gives the whole process flowchart and then demonstrates in a practical distribution network. Section VII draws conclusions.

II. The Concept of the Proposed Framework

Since FLR uncertainties seriously affect traditional investment decision-making, network owners have an incentive to postpone commitment and wait for new information to avoid costly investment mistakes. There are three challenges here, 1) evaluating waiting time, 2) quantifying waiting profit, and 3) quantifying waiting cost.

The proposed idea of reflecting uncertainty in decision making is shown in Fig.1. Firstly, corresponding to nodal FLR uncertainty, the combined cumulant and Gram-Charlier expansion method is applied to convert nodal uncertainty to the branch probabilistic power flows. The TRH of the network is determined by the peak of branch power flow. It then dynamises the network TRH via 'wait and see', which means the TRH under uncertainty is determined by the trade-off between cost and profit resulted from waiting. The waiting profit, representing the benefits of deferring the investment, is quantified by the present value difference. The waiting cost, reflecting the cost due to waiting, is evaluated by the options' cost based on real options method. Then, calculated via the Sharpe ratio and the expected return, the investment decision is determined by providing the waiting time, reflected as the length of investment deferral horizon.

Fig.1. The solution of reflecting uncertainty in decision making.

III. Probabilistic Power Flow with Demand and Generation Uncertainty

To reflect the FLR uncertainties into the system peak-based investment decision, probabilistic power flow is proposed to convert the nodal uncertainties to branch power flow uncertainty by using combined cumulant and Gram-Charlier expansion methods.

A. Power Flow Linearisation

For probabilistic power flow analysis, a linear combination of independent variables is considered in the cumulant method. In the distribution network, especially radial ones, the DistFlow model [29, 30] is widely used to simplify the relationship between nodal power change and branch power flow, which is modelled as:

$$P_{l+1} = P_l - \frac{r_l \times (P_l^2 + Q_l^2)}{V_l^2} - p_{i,l} \tag{1}$$

$$Q_{l+1} = Q_l - \frac{x_l \times (P_l^2 + Q_l^2)}{V_l^2} - q_{i,l} \tag{2}$$

$$V_{l+1}^2 = V_l^2 - 2(r_l \times P_l + x_l \times Q_l) + \frac{(P_l^2 + Q_l^2)(r_l^2 + x_l^2)}{V_l^2} \tag{3}$$

where P_l and Q_l are active and reactive power flows on branch l; the branch impedance is presented as $z_l = r_l + jx_l$.

Nodal voltages in distribution networks should be within a certain range to comply with security standard, set as $V_l \subset [0.95, 1.05]$. Since the linear part of the nodal voltage are much larger than the nonlinear part, $(P_l^2 + Q_l^2)(r_l^2 + x_l^2)/V_l^2$ can be ignored [30, 31]. By assuming nodal voltage at the nominal level is $1\ \text{p.u.}$, $(V_l - 1)^2 = V_l^2 - 2V_l + 1 \approx 0$, then $V_l^2 \approx 2V_l + 1$. It can yield $V_{l+1} = V_l - (r_l P_l + x_l Q_l)$ from $2V_{l+1} - 1 = 2V_l - 1 - 2(r_l P_l + x_l Q_l)$ based on (3).

Thus, the DistFlow model can be simplified as:

$$P_{l+1} = P_l - p_{n,l} \tag{4}$$

$$Q_{l+1} = Q_l - q_{n,l} \quad (5)$$

$$V_{l+1} = V_l - (r_l \times P_l + x_l \times Q_l) \quad (6)$$

where $p_{n,l}$ and $q_{n,l}$ represent the active and reactive power injection at the node n along branch l.

Therefore, branch flow change due to nodal power change can be determined according to linearised DistFlow. Inspired by power transfer distribution factor, an index matrix ($M_{n,l}$) is determined by the sensitivity of an injected nodal power on the changing branch power flow in (7), which is used to measure the impact of the located at node n on branch l's flow.

$$M_{n,l} = \frac{\partial P_l}{\partial p_{n,l}} \quad (7)$$

B. Cumulant Method

The combined cumulant and Gram-Charlier expansion method are used to formulate the probabilistic power flow with uncertainties. In probability density function (PDF), cumulants and moments can characterise its feature. The mean is the first order cumulant and variance is the second-order cumulant of the distribution. For a random variable x, such as load at node n, i.e. P_n, the moment generating function $\Phi_{P_n}(s)$ is:

$$\Phi_{P_n}(s) = E[e^{sP_n}] = \int_{-\infty}^{\infty} e^{sP_n} f_{P_n}(P_n)\, dP_n \quad (8)$$

where $f_{P_n}(P_n)$ is the PDF of P_n.

The cumulant generating function $\Psi_{P_n}(s)$ can be determined by the moment generating function:

$$\Psi_{P_n}(s) = \ln \Phi_{P_n}(s) \quad (9)$$

The *n-th* order raw moment m_n and cumulant λ_n can be determined at s=0, which can be calculated by taking the *n*-th derivative of the moment and cumulant generating function. Variable P_l is the active power flow on branch l, which can be aggregated by the linear combination of independent load at different nodes (P_{n_1}, P_{n_2} ... P_{n_m}), as follows:

$$P_l = M_{1,l}P_{n_1} + M_{2,l}P_{n_2} + \cdots M_{m,l}P_{n_m} \quad (10)$$

Hence, its moment generating function can be determined as:

$$\begin{aligned}\Phi_{P_l}(s) &= E[e^{sP_l}] = E\left[e^{s(M_{1,l}P_{n_1} + M_{2,l}P_{n_2} + \cdots M_{m,l}P_{n_m})}\right] \\ &= E\left[e^{s(M_{1,l}P_{n_1})s(M_{2,l}P_{n_2}) + \cdots s(M_{m,l}P_{n_m})}\right] \\ &= \Phi_{P_{n}1}(M_{1,l}s)\Phi_{P_{n}2}(M_{2,l}s) \ldots \Phi_{P_{n}m}(M_{m,l}s)\end{aligned} \quad (11)$$

where $M_{n,l}$ is the linearised power flow index between nodal load and branches, determined by (7).

Thus, the cumulant for variable P_n is:

$$\begin{aligned}\Psi_{P_l}(s) &= ln(\Phi_{P_l}(s)) \\ &= \Psi_{P_{n_1}}(a_1 s) + \Psi_{P_{n_2}}(a_2 s) + \cdots \Psi_{P_{n_m}}(a_m s)\end{aligned} \quad (12)$$

The *n*th-order cumulant of P_l can be calculated by taking the *n*th derivative of $\Psi_{P_l}(s)$ respective to s at $s = 0$.

$$\begin{aligned}\lambda_n &= \Psi_{P_l}^{(n)}(0) \\ M_1^n\Psi_{P_{n_1}}^{(n)}(0) &+ M_2^n\Psi_{P_{n_2}}^{(n)}(0) + \cdots M_m^n\Psi_{P_{n_m}}^{(n)}(0)\end{aligned} \quad (13)$$

C. Gram-Charlier Expansion Method

Combined with the moment of load PDF generated from Section II.B, the Gram-Charlier expansion method is implemented, which aggregates nodal PDFs as a series composed of a standard normal distribution and derivatives. By applying Edgeworth form, the Gram-Charlier form can be determined by moments and cumulants, considering the additive property of cumulants. Thus, the exponential representation of the PDF can be calculated based on the cumulants of distribution in the standard form, in (14-15).

$$f(P_n) = e^{(-\frac{\lambda_3}{3!}D^3 + \frac{\lambda_4}{4!}D^4 - \frac{\lambda_5}{5!}D^5 + \cdots)}\beta(P_n) \quad (14)$$

$$\beta(P_n) = \frac{1}{\sqrt{2\pi}\sigma} e^{-\frac{(P_n-\mu)^2}{2\sigma^2}} \quad (15)$$

where D^n is the *n*-th order derivative of the unit normal distribution, $\beta(P_n)$ is the normal distribution function with the mean (μ) and variance (δ), λ_n is the *n*-th order cumulant. In the normal distribution, the 1st order cumulant is μ and the 2nd order cumulant is δ^2.

Thus, the exponential series is:

$$\begin{aligned}f(P_n) = \Bigg[1 &+ \frac{(-\frac{\lambda_3}{3!}D^3 + \frac{\lambda_4}{4!}D^4 - \frac{\lambda_5}{5!}D^5 + \cdots)}{1!} + \frac{(-\frac{\lambda_3}{3!}D^3 + \frac{\lambda_4}{4!}D^4 - \frac{\lambda_5}{5!}D^5 + \cdots)^2}{2!} + \\ &\frac{(-\frac{\lambda_3}{3!}D^3 + \frac{\lambda_4}{4!}D^4 - \frac{\lambda_5}{5!}D^5 + \cdots)^3}{3!} + \cdots \Bigg]\beta(P_n)\end{aligned} \quad (16)$$

By expanding each term and grouping by the power of D, the PDF can be expressed as:

$$\begin{aligned}f(P_n) &= \beta(P_n) - \frac{\lambda_3}{3!}D^3\beta(P_n) + \frac{\lambda_4}{4!}D^4\beta(P_n) - \frac{\lambda_5}{5!}D^5\beta(P_n) + \\ &\left(\frac{\lambda_6}{6!} + \frac{\lambda_3{}^2}{2!3!^2}\right)D^6\beta(P_n) - \left(\frac{\lambda_7}{7!} + \frac{2\lambda_3\lambda_4}{2!3!4!}\right)D^7\beta(P_n) + \cdots\end{aligned} \quad (17)$$

IV. NETWORK INVESTMENT DECISION-MAKING MODEL

In this paper, the waiting time is determined by the Sharpe ratio, evaluated by waiting cost, expected return, and risk level resulting from FLR uncertainty.

A. Waiting time horizon

To evaluate the waiting time horizon, the Sharpe ratio is introduced based on the expected return and risk at the year after investment deferral. The expected return is derived according to the waiting cost and waiting profit. With the Sharpe ratio (SR_t) of each year in (19), TRH (n_l) in (18) is the maximum period with the positive Sharpe ratio over time, delivered as follows:

$$n_l = max\, t \qquad (SR_t > 0) \quad (18)$$

$$SR_t = \frac{Rr_t - Rf}{\sigma_t} \tag{19}$$

$$Rr_t = \frac{Pt_t - Wc_t}{Wc_t} \tag{20}$$

where Rr_t is the return of deferring investment; Rf is the risk-free rate; σ_t is the standard deviation of the return, which is determined by the risk level; Pt_t is the waiting profits and Wc_t is the waiting cost resulting from deferring to year t.

Normally, the Sharpe ratio should be positive, which means the profit is higher than the risk-free rate. If the Sharpe ratio is smaller than zero, it is meaningless to analyse it.

B. The profits from waiting

Since the current investment cost is reserved for n_l years by paying the waiting cost, the profit is the present value difference between now (PV_0) and year n_l (PV_{n_l}) [7].

$$PV_0 = \frac{Asset_l}{(1+r)^{\frac{\log C_l - \log P_l}{\log(1+g_l)}}} \tag{21}$$

$$PV_{n_l} = \frac{Asset_l}{(1+dr)^{\frac{\log C_l - \log P_l}{\log(1+g_l)}+n_l}} \tag{22}$$

$$Pt_t = PV_{n_l} - PV_0 \tag{23}$$

where $Asset_l$ is the asset cost, r is the discount rate, C_l is the capacity, P_l is the peak power flow level and g_l is the load growth rate for branch l.

C. The waiting cost

To obtain more information about future FLR change, network owners would like to pay the waiting cost if it is less than the waiting profit. onsidering the impact of uncertainty, the present value of the anticipated stream cash flow (V_0) is:

$$V_0 = -c + \frac{1}{1+r}R_0 + \left[\frac{1}{1+r}\right]^2 \sum_{i=0}^{\infty}(1-r)^{-i}\,E_0[R] \tag{24}$$

the present value in one year later is:

$$V_1 = Pr[R > rc]\{\frac{-c}{1+r} + \left[\frac{1}{1+r}\right]^2 \sum_{i=0}^{\infty}(1-r)^{-i}\,E_0[R|R > rc] \tag{25}$$

Thus, the waiting cost is the difference between V_0 and V_1, which is:

$$Wc_1 = \left(\frac{1}{1+r}\right)[Pr[R > rc]\frac{E_0[rc - R|R < rc]}{r} - (R_0 - rc) \tag{26}$$

However, for the waiting cost in year n_l, it should recurse n_l times, which is too complex and not accurate to evaluate the uncertain return. Thus, with real options concept, the waiting cost is determined by the cost of options of the uncertainty, which means the current investment cost can be reserved until the year n_l by paying the waiting cost.

D. The real options method

The real options method is developed based on the risk-neutral theory. It is explained by the binomial options pricing method [11], which uses binomial lattice (tree) to determine the value of the options during a number of time steps from the current time to the ending time. Each node in the tree represents a possible present value of the asset at a given time step, which is a called term and assumed to be one year in this paper.

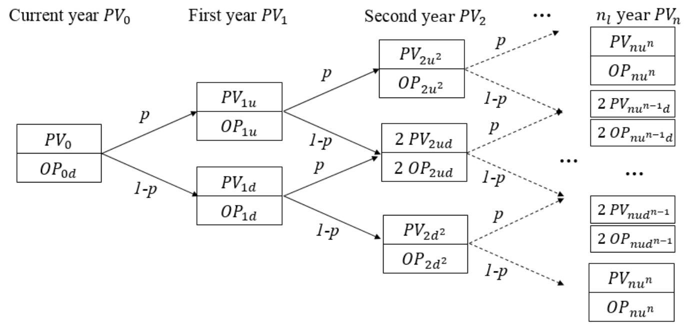

Fig.2. The binomial tree for year N.

Starting from the final nodes (the step at left side treetop), it calculates backwards towards the first node (the right side root of the tree), as shown in Fig.2. For the first-year case, the present value of an asset in the current year is PV_0. It will grow by u times, in (28), to PV_{1u} with a probability of p or decrease by d times, in (29), to PV_{1d} with a probability of $1-p$ one year later, shown in (27). The options for the probability present asset value increase and decrease at the final node (one year later) are OP_{1u} and OP_{1d}, respectively, in (30-31). The risk-neutral method in (32) evaluates the value of the options at the final node by assuming that the present value in one year later (PV_1) is constant, regardless of the risk. The probability of present value change over time can be derived from (27-32) in (33). Then, for network operators, the options' cost in the current year (OP_0) in (34) can be discounted from the final node based on the riskless interest rate r_r [11].

$$PV_1 = PV_{1u} \times p + PV_{1d} \times (1-p) \tag{27}$$

$$u = \frac{PV_{1u}}{PV_0} \tag{28}$$

$$d = \frac{PV_{1d}}{PV_0} \tag{29}$$

$$OP_{1u} = max(0, PV_{1u} - PV_1) \tag{30}$$

$$OP_{1d} = max(0, PV_{1d} - PV_1) \tag{31}$$

$$PV_{1u} - OP_{1u} = PV_{1d} - OP_{1d} = PV_1 \tag{32}$$

$$p = \frac{e^{-rt} - d}{u-d} \tag{33}$$

$$\begin{aligned} OP_0 &= e^{-rt} \times [OP_{1u} \times p + OP_{1d} \times (1-p)] \\ &= e^{-rt} \times [\frac{e^{r_r t} - d}{u-d} \times OP_{1u} + \frac{u - e^{r_r t}}{u_0 - d} \times OP_{1d}] \end{aligned} \tag{34}$$

where, specific factors u and d depict the present value change in the current year to the next year; r_r is the riskless interest rate over one period, and t is the length of the period.

For the waiting horizon n_l, with the options' value at n_l, the options' value at year $n_l - 1$ can be calculated. After n_l times recursive, the options' value at the current year can be determined from (27-34). This procedure is shown in Fig.2 and explained in (35).

$$OP_0 = e^{-r_r t} \times \left[\sum_{i=0}^{n} \frac{n_l!}{i! \times (n_l - i)!} \times p^i \times (1-p)^{n_l - i} \times \Delta PV\right] \quad (35)$$

V. The Implementation Process

To determine the optimal TRH and the waiting cost under uncertainty, the whole implementation procedure contains two key stages, which are capturing uncertainty and reflecting uncertainty in the decision-making progress. The flow chart is depicted in Fig.3.

A. Stage 1: Capturing uncertainty

By using the combined cumulant and Gram-Charlier expansion method, the FLR uncertainties are converted into probabilistic power flow uncertainty according to the forecasting error based on Equations (1-17). The forecasting error increases over time, evaluated by the triple exponential smoothing method.

Simultaneously, the TRH and the present value of branches can be calculated by the current discount cash flow model. Based on current loading level and load growth rate, the unused capacity of different branches is used to evaluate the TRH and present value without uncertainty. These values are set as the references in the case considering uncertainty.

B. Stage 2: Reflecting uncertainty

With the present value of branches, the time horizon to waiting and waiting cost can be determined year by year. The expected return is the difference between waiting profit in Equations (21-23) and waiting cost. To accurately evaluate the uncertain return over time, the waiting cost is represented by the options' cost in Equations (27-35). If the return is positive, it means the network owner can get benefit from investment decision-making deferral. The maximum time to defer is determined by expected return before the return become negative, which means the Sharpe ratio at this year should be positive. The TRH of each branch is the maximum of deferred time with positive Sharpe ratios in Equations (18-20).

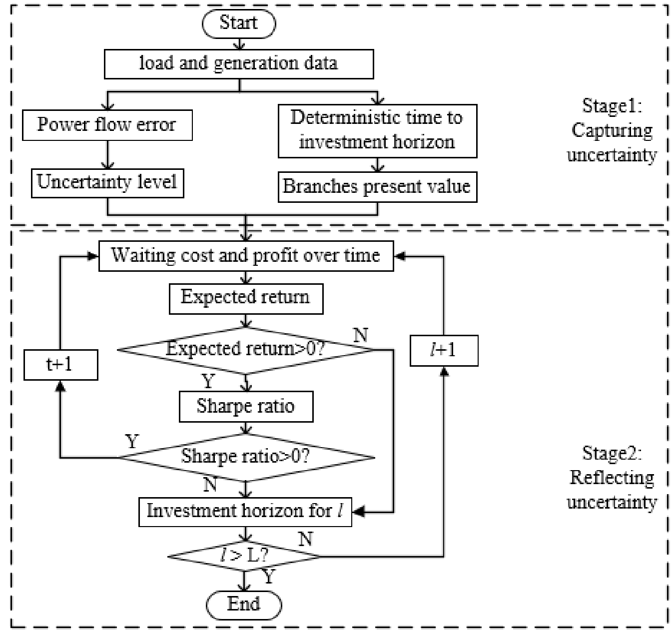

Fig. 3. Flowchart for the whole process

VI. Practical Network Demonstration

The proposed decision-making scheme is demonstrated on a practical local Grid Supply Point area in the UK in Fig.4 [32]. The asset lifespan of the system is 40 years and annuity factor is 0.0831 [7]. A typical load growth of 2% and a discount rate of 5.6% are chosen. A wind generation (G1) is located at bus 1005, with a peak output of 5MW. The photovoltaic generation in branch 1016 has peak power output 5MW. The upstream system, at slack bus 1008, is modelled as G1008.

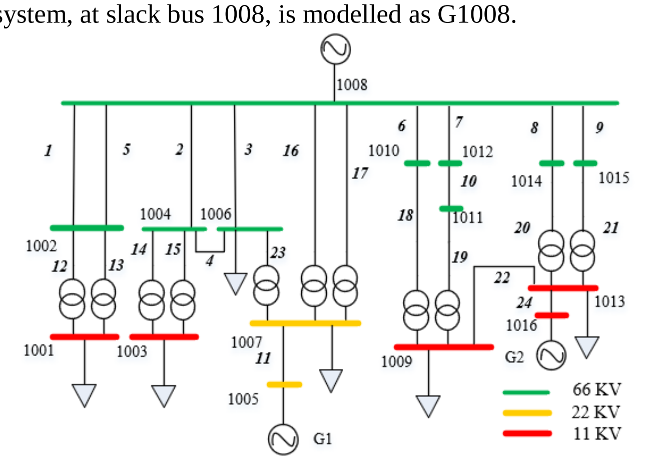

Fig.4. A Grid Supply Point area test system.

The capacity and asset cost are listed in Table I. The branches No.2&3 have large capacity 54.5MW. The branch No.2 has the highest asset cost, i.e. £1.85 billion. Branch No.23 is the interconnector between two areas, which has the capacity of 15.0MW. The branches with transforms have the same cost, which is £0.44billion.

TABLE I
The capacity of each branch (MW)

Branch	Asset cost (£b)	Capacity (MW)	Branch	Asset cost (£b)	Capacity (MW)

No.1	1.60	45.0	No.14	0.44	32.0
No.2	1.85	54.5	No.15	0.44	32.0
No.3	1.48	54.5	No.16	0.44	32.0
No.4	0.32	15.0	No.17	0.44	32.0
No.5	1.60	45.0	No.18	0.44	15.0
No.6	1.75	30.0	No.19	0.44	15.0
No.7	1.75	30.0	No.20	0.44	15.0
No.8	0.45	30.0	No.21	0.44	15.0
No.9	0.60	30.0	No.22	0.44	15.0
No.10	1.17	15.0	No.23	0.44	15.0
No.11	0.32	10.0	No.24	0.44	15.0

A. The uncertainty level of the future

The uncertainty levels of the load and demand are determined by the standard deviation of the forecast errors based on triple exponential smoothing method. The FLR uncertainty resulting from forecast error are aggregated from nodes to branch power flow error based on the combined cumulant and Gram-Charlier expansion method. Fig. 5 shows the distributions of power flow forecast error on branch No.2 in 1-year, 10-year and 20-year ahead, with the standard deviation of 0.09, 0.16 and 0.38, respectively. It demonstrates that the accuracy of load forecasting decreases as the TRH increases. With shorter TRH, the forecasted value has more concentrated error distribution around zero, which indicates that the forecasted value is more accurate and reliable. With a larger TRH, the forecasted value has more flat distribution, which implies that the predicted results are more scattered and less accurate.

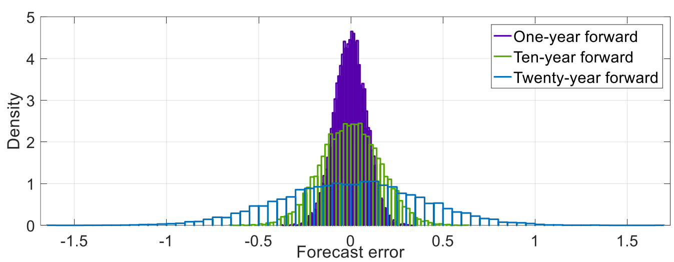

Fig.5. Distribution of load forecasting error for branch flow on No.2

The standard deviation of different branch flows resulting from FLR forecasting error is shown in Fig.6. The branches No.11, 14 and 15 have the highest uncertainty resulting from more FLR on connected nodes, which nodal uncertainty is more significant to impact the power flows on nearby branches.

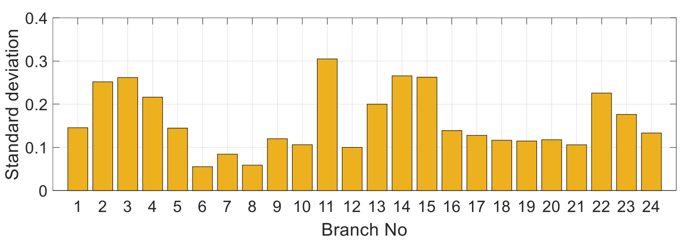

Fig.6. The forecasting error for different branch flow

B. Expected returns and waiting cost

Corresponding to the uncertainty of peak power flows, the waiting profit and waiting cost are determined by the present value change and options cost resulting from investment decision deferral of different branches.

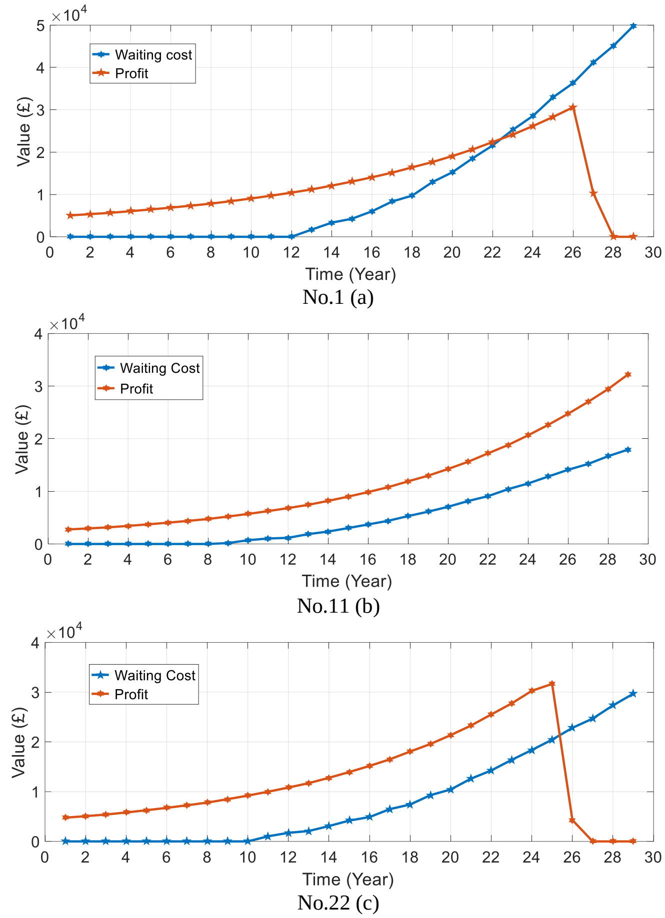

Fig.7. The waiting cost and profit for different branches over time

The waiting cost and waiting profit due to the decision-making investment deferral on branches No.1, No.11, and No.22 are depicted respectively in Fig.7(a-c). Corresponding to the peak point on the profit curve, the branch investment time is determined by the original decision-making tool without considering uncertainty. These three figures represent three typical results of the proposed method based on the trade-off between the waiting cost and profits. Fig.7(a) describes the waiting cost and profit on branch No.1 overtime. The forecast error on branch No.1 is from the nodal load on busbar 1001, which uncertainty is small. The waiting cost at year 20 is £16k, which is smaller than the profit (£20k). These two values are equal to £21k at year 22 and the waiting cost will be larger than the profits after year 22, which means the reinforcement should not be deferred on this branch. Branch No.11 has higher waiting profits than the waiting cost with the investment deferral, shown in Fig.7(b). Since this branch is connected to the renewables on busbar 1005, to the uncertainty level of branch peak power flow is high. The future investment cost reduction is more than the profit increase, which is because of the uncertainty reduction and sufficient spare branch capacity to absorb the impact of uncertainty. The profit on this branch is £14k at year 10, which is much higher than the waiting cost £8k. The profit is bigger than the waiting cost over the analysed period due to its high uncertainty level, which means waiting is more valuable on this branch. Fig.7(c) shows results on branch

No.22. The profit is higher than the waiting cost until year 25.5, around £22k, which means the branch must be reinforced after this time.

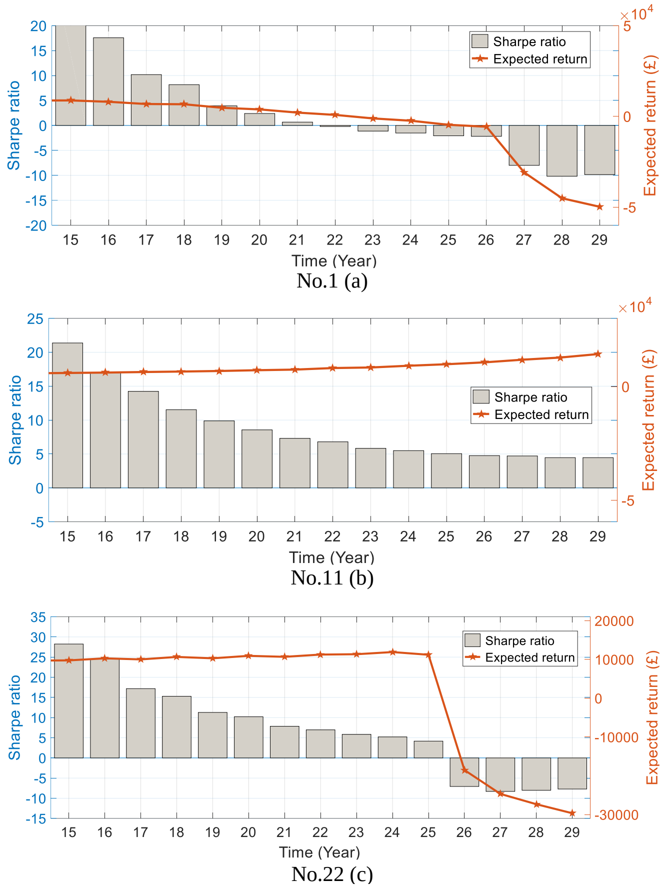

Fig.8. Expected return and Sharpe ratio for different branches over time

Corresponding to the waiting cost and profits in Fig.7(a-c), the expected return and the Sharpe ratio of these branches are depicted in Fig.8(a-c). On branch No. 1, the waiting cost is higher than the profit after year 22, which means the expected return is negative after this year in Fig.8(a). Thus, the TRH is forwarded due to the limited capacity of this branch, which should be reinforced at current rather than waiting. On branch No.11, since the waiting profit is higher than the waiting cost, the expected return is positive, shown in Fig.8(b). Since the expected return is positive and the Sharpe ratio is increasing slightly over time, the system still can get benefit from deferring the investment. Thus, the investment on this branch should be deferred and should wait for more information for more accurate decision. On branch No.22, the profit is higher than the waiting cost until year 25.5, which means the expected return of this branch is positive before year 26. The Sharpe ratio, is also positive until year 26, which means the TRH can be deferred by half a year.

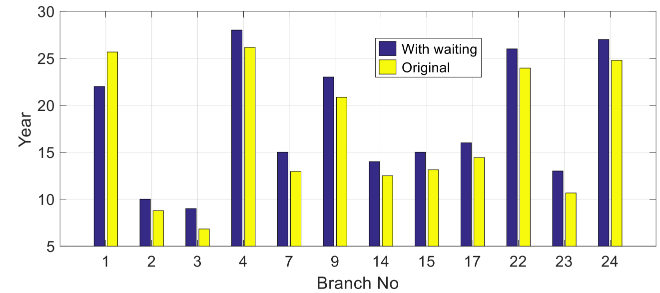

Fig.9. Time to reinforcement horizon (TRH)

Fig.9 describes the TRH change under different scenarios on different branches. The original scenario of TRH is calculated based on the traditional decision-making method without considering the uncertainty. Since the maximum value of peak probabilistic power flow is used in the traditional method, it is more likely to get a lower peak in practice if the uncertainty level is high. Based on the uncertainty level and the unused capacity of the branches, the results show that the majority of the branches are impacted essentially by the uncertainty. Thus, it is better to defer investment for more information until the uncertainty is reduced. For the branches with small uncertainty level and limited unused capacity, represented by No.1, the TRH is shortened. The investment should be deferred on the majority of branches to reduce the impact of uncertainty. For example, the TRH of branch No.3 is deferred 3.2 years, which is from 6.8 years to 10 years.

C. Sensitivity analysis

Since the uncertainty poses a significant impact to the waiting cost and the TRH, the sensitivity analysis is provided corresponding to different uncertainty levels. Table II provides the sensitivity analysis on waiting cost on branch No.16. With the uncertainty level increase, the waiting cost is increasing less swiftly. If the waiting horizon is 8 years, the waiting cost is £7.0k with current uncertainty level. It will increase to £8.1k if the uncertainty level increases by 20% and it will decrease to £6.0k if the uncertainty level reduces by 20%.

TABLE II: The waiting cost of different uncertainty level (£k)

Scenario \ Year	3	8	13	18	20
-20% uncertainty	0.4	6.0	12.4	18.4	20.3
Original	1.0	7.0	13.7	19.8	21.6
+20% uncertainty	1.5	8.1	15.2	21.2	22.7

The sensitivity analysis of waiting cost and profit is depicted in Fig.10. The solid line represents the profits and the dashed line is the waiting cost of different scenarios. With higher uncertainty level, the profit and the waiting cost are increasing. With positive Sharpe ratios, the intersection of profit and waiting cost can represent the TRH. The TRH is 26 years without considering the impact of FLR uncertainty. At the current uncertainty level, the TRH is 26.8 year in the blue curves via the proposed method, which defers 0.8-year than the TRH via the traditional method. With 20% uncertainty level reduction, the TRH changes to 26.3 years. It defers 1.8 more years to 27.8 years if the uncertainty level increases by 20%.

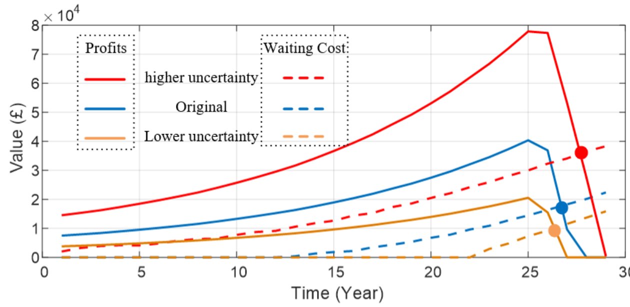

Fig.10. Profits and waiting cost for different branches over time No.24

VII. Conclusions

This paper designs a decision-making scheme for network operators to capture the uncertainty in future system investment. Through extensive demonstration, the following key findings are obtained:

- The proposed method efficiently determines the time to waiting horizon under uncertaint, which dynamises the network investment time and reduces the impact of uncertainty.
- Paying waiting cost provides an alternative way for network owners instead of investment under uncertaint, reduc risk and cost simultaneously;
- With significant , it is more to defer investment and wait for more information to reduce the impact of uncertaint.

This work helps network operators avoid irreversible investment, particularly with fast-growing energy storage and electric vehicle, which could reduce the requested transmission capacity. t provides an economic solution for network operators to address uncertainties in the future system.

References

[1] I. E. Agency, "IEA: Renewable electricity set to grow 40% globally by 2022," https://www.carbonbrief.org/iea-renewable-electricity-set-to-grow-40-globally-by-2022, 2017.

[2] BusinessGreen, "UK energy storage tipped to exceed 1.6GW by 2020," http://www.businessgreen.com/bg/analysis/2442158/uk-energy-storage-tipped-to-exceed-16gw-by-2020, 2016.

[3] O. energi, "HOW EVS CAN HELP DRIVE A MORE SUSTAINABLE ENERGY FUTURE," https://www.openenergi.com/evs-can-help-fuel-sustainable-energy-future/, 2017.

[4] L. Pieltain Fernandez, "Assessment of the Impact of Plug-in Electric Vehicles on Distribution Networks," *IEEE Transactions on Power Systems,* vol. 26, no. 1, pp. 206-214, 2011.

[5] D. W. Jorgenson, "CAPITAL THEORY AND INVESTMENT BEHAVIOR," *American Economic Review,* vol. 53, no. 2, pp. 247-260, 1963.

[6] J. Tobin, "A General Equilibrium Approach To Monetary Theory," *Journal of Money, Credit & Banking (Ohio State University Press),* vol. 1, no. 1, pp. 15-30, 1969.

[7] F. Li and D. L. Tolley, "Long-run incremental cost pricing based on unused capacity," *Power Systems, IEEE Transactions on,* vol. 22, no. 4, pp. 1683-1689, 2007.

[8] T. Ding, S. Liu, W. Yuan, Z. Bie, and B. Zeng, "A Two-Stage Robust Reactive Power Optimization Considering Uncertain Wind Power Integration in Active Distribution Networks," *IEEE Transactions on Sustainable Energy,* vol. 7, no. 1, pp. 301-311, 2016.

[9] J. A. Miles and J. R. Ezzell, "The Weighted Average Cost of Capital, Perfect Capital Markets, and Project Life: A Clarification," *The Journal of Financial and Quantitative Analysis,* vol. 15, no. 3, pp. 719-730, 1980.

[10] W. Ding and R. Z. Cao, "An approach to calculate the value of a company," in *Proceedings of 2011 IEEE International Conference on Service Operations, Logistics and Informatics*, 2011, pp. 89-94.

[11] J. C. Cox, S. A. Ross, and M. Rubinstein, "Option pricing: A simplified approach," *Journal of financial Economics,* vol. 7, no. 3, pp. 229-263, 1979.

[12] M. Tahon *et al.*, "Real Options in Telecom Infrastructure Projects — A Tutorial," *IEEE Communications Surveys & Tutorials,* vol. 16, no. 2, pp. 1157-1173, 2014.

[13] B. Zou, J. Wang, and F. Wen, "Optimal investment strategies for distributed generation in distribution networks with real option analysis," *IET Generation, Transmission & Distribution,* vol. 11, no. 3, pp. 804-813, 2017.

[14] D. Liu, G. Li, N. Hu, and Z. Ma, "Application of Real Options on the Decision-Making of Mining Investment Projects Using the System Dynamics Method," *IEEE Access,* vol. 7, pp. 46785-46795, 2019.

[15] L. Kauppinen, A. S. Siddiqui, and A. Salo, "Investing in Time-to-Build Projects With Uncertain Revenues and Costs: A Real Options Approach," *IEEE Transactions on Engineering Management,* vol. 65, no. 3, pp. 448-459, 2018.

[16] J. A. Schachter and P. Mancarella, "Demand Response Contracts as Real Options: A Probabilistic Evaluation Framework Under Short-Term and Long-Term Uncertainties," *IEEE Transactions on Smart Grid,* vol. 7, no. 2, pp. 868-878, 2016.

[17] A. C. Passos, A. Street, and L. A. Barroso, "A Dynamic Real Option-Based Investment Model for Renewable Energy Portfolios," *IEEE Transactions on Power Systems,* vol. 32, no. 2, pp. 883-895, 2017.

[18] R. S. Pindyck, "LECTURES ON REAL OPTIONS: PART I—BASIC CONCEPTS," *Dostupné z:* http://web. *mit. edu/rpindyck/www/Courses/RO_P1_Handout% 20Slides. pdf,* 2008.

[19] X. Yan, C. Gu, F. Li, and Y. Xiang, "Network pricing for customer-operated energy storage in distribution networks," *Applied Energy,* vol. 212, pp. 283-292, 2018/02/15/ 2018.

[20] C. Gu, J. Wu, and F. Li, "Reliability-Based Distribution Network Pricing," *IEEE Transactions on Power Systems,* vol. 27, no. 3, pp. 1646-1655, 2012.

[21] D. T. Wang, L. F. Ochoa, and G. P. Harrison, "DG Impact on Investment Deferral: Network Planning and Security of Supply," *IEEE Transactions on Power Systems,* vol. 25, no. 2, pp. 1134-1141, 2010.

[22] A. K. Dixit, R. K. Dixit, R. S. Pindyck, and R. Pindyck, *Investment under uncertainty*. Princeton university press, 1994.

[23] W. Setiawan, E. Juniati, and I. Farida, "The use of Triple Exponential Smoothing Method (Winter) in forecasting passenger of PT Kereta Api Indonesia with optimization alpha, beta, and gamma parameters," in *2016 2nd International Conference on Science in Information Technology (ICSITech)*, 2016, pp. 198-202.

[24] S. Dev, T. AlSkaif, M. Hossari, R. Godina, A. Louwen, and W. v. Sark, "Solar Irradiance Forecasting Using Triple Exponential Smoothing," in *2018 International Conference on Smart Energy Systems and Technologies (SEST)*, 2018, pp. 1-6.

[25] X. Yan, C. Gu, H. Wyman-Pain, and F. Li, "Optimal Capacity Management for Multi-Service Energy Storage in Market Participation using Portfolio Theory," *IEEE Transactions on Industrial Electronics,* pp. 1-1, 2018.

[26] L. Zhou, F. Li, and X. Tong, "Active Network Management Considering Wind and Load Forecasting Error," *IEEE Transactions on Smart Grid,* vol. 8, no. 6, pp. 2694-2701, 2017.

[27] S.-N. Chen and H. Jang, "On selectivity and market timing ability of US-based international mutual funds: Using refined Jensen's measure," *Global Finance Journal,* vol. 5, no. 1, 1994.

[28] G. Hübner, "The generalized Treynor ratio," *Review of Finance,* vol. 9, no. 3, pp. 415-435, 2005.

[29] M. E. Baran and F. F. Wu, "Network reconfiguration in distribution systems for loss reduction and load balancing," *IEEE Transactions on Power delivery,* vol. 4, no. 2, pp. 1401-1407, 1989.

[30] L. Bai, J. Wang, C. Wang, C. Chen, and F. F. Li, "Distribution Locational Marginal Pricing (DLMP) for Congestion Management and Voltage Support," *IEEE Transactions on Power Systems,* 2017.

[31] H.-G. Yeh, D. F. Gayme, and S. H. Low, "Adaptive VAR control for distribution circuits with photovoltaic generators," *IEEE Transactions on Power Systems,* vol. 27, no. 3, pp. 1656-1663, 2012.

[32] C. Gu, F. Li, and Y. He, "Enhanced long-run incremental cost pricing considering the impact of network contingencies," *Power Systems, IEEE Transactions on,* vol. 27, no. 1, pp. 344-352, 2012.